MNRAS **000**, 1–10 (2020) Preprint 12 January 2021 Compiled using MNRAS LATEX style file v3.0

Warm millimetre dust in protoplanetary discs near massive stars

Thomas J. Haworth[1]★

[1] *Astronomy Unit, School of Physics and Astronomy, Queen Mary University of London, London E1 4NS, UK*

Accepted ???. Received ???; in original form ???

ABSTRACT

Dust plays an extremely important role in the formation of planets and its emission also provides one of our most accessible views of protoplanetary discs. The temperature of this dust is usually assumed to be set by radiative equilibrium with the central star, plateauing at around 10–20 K in the outer disc. However many stars form in clusters where stellar neighbours can play an appreciable role in heating dust throughout the disc. In this paper we study the radiative equilibrium temperature of discs in the presence of external sources. In particular we are interested in the effect that increased disc heating from external sources has on millimetre dust mass estimates. Since large grains are not entrained in any wind we hence focus on geometrically simple 2D-axisymmetric disc models with radiative transfer calculations that consider both the host star and an external source. In assuming a disc temperature of 20 K for a disc a distance D from a strong radiation source, disc masses are overestimated by a factor that scales with $D^{-1/2}$. This could significantly alter disc mass estimates of discs in close proximity to θ^1C in the Orion Nebular Cluster. We also make an initial assessment of the effect upon snow lines. Within a parsec of an O star like θ^1C a CO snow line no longer exists, though the water snow line is virtually unaffected except for very close separations of ≤ 0.01 pc.

Key words: accretion, accretion discs – circumstellar matter – protoplanetary discs – hydrodynamics – planetary systems: formation – photodissociation region (PDR)

1 INTRODUCTION

Although we have known about the impact of environment on circumstellar discs essentially for as long as we have been able to directly image them (O'dell & Wen 1994), there has recently been a resurgence of interest in the topic.

The three main ways that environment affects discs is through external photoevaporation, dynamical (gravitational) encounters and through compositional inheritence and enrichment (e.g. of short lived radionuclides like Aluminium 26, Lichtenberg et al. 2019; Reiter 2020, though we do not focus on this here). Recent developments with regard to the first two points include a better understanding the effect of dynamics and external photoevaporation in different types of stellar cluster (Scally & Clarke 2001; Winter et al. 2018; Concha-Ramírez et al. 2019; Nicholson et al. 2019) which were facilitated by improvements in external photoevaporation models (Haworth et al. 2018b; Haworth & Clarke 2019), observations of interacting systems (e.g. Rodriguez et al. 2018; Kurtovic et al. 2018) and an ever increasing catalogue of photoevaporating discs (e.g. Kim et al. 2016; Haworth et al. 2020). The recent linking of possibly distinct exoplanet populations in Gaia phase space overdensities also provides a tantalizing hint of the impact of environment (at the formation stage, or over a longer period of time) on the resulting planets themselves (Winter et al. 2020).

Another extremely powerful recent development stems from the unprecedented sensitivity and resolution that ALMA provides. ALMA surveys of discs in clusters now allow us to analyse disc statistics throughout star forming regions (e.g. Mann et al. 2014; Ansdell et al. 2017; Eisner et al. 2018; Boyden & Eisner 2020; Ansdell et al. 2020). In particular, trends in disc properties as a function of projected separation from the strongest UV sources is often interpreted as evidence for external photoevaporation (Mann et al. 2014; Ansdell et al. 2017; Eisner et al. 2018). However, the dynamical evolution of the cluster can drastically complicate this picture (Parker et al. in preparation). Nevertheless trends do remain, most commonly trends in the dust properties (mass, radius), that require an explanation.

The most accessible (i.e. least demanding in terms of observing time) insight into the disc properties with ALMA comes from estimating the dust mas from the measured continuum flux F_ν. This is done by integrating the formal solution to the equation of radiative transfer in the limit of constant absorption and emission coefficient, no background source and dust emitting as a blackbody (Planck function B_ν)

$$I_\nu = B_\nu \left(1 - \exp(-\tau_\nu)\right) \quad (1)$$

over the beam solid angle Ω_B to convert the emergent intensity I_ν

★ E-mail: t.haworth@qmul.ac.uk

to a flux F_ν

$$F_\nu \approx B_\nu \tau_\nu \Omega_B = B_\nu \kappa_\nu \rho l \Omega_B. \quad (2)$$

The solid angle is then related to the mass

$$M_d = \rho l \Omega_B D^2 \quad (3)$$

hence

$$M_d = \frac{D^2 F_\nu}{\kappa_\nu B_\nu(T)} \quad (4)$$

is the well known expression used to estimate dust masses from a measured flux F_ν. This relies upon an assumed distance D, opacity at the frequency of observation κ_ν and dust temperature T. Generally this dust temperature is assumed to be 20 K, which probably applies well to nearby discs to the Sun which are very extended (hundreds of au in size) and expected to be relatively cold over the bulk of the disc mass. Tazzari et al. (2017) validated this further with UV plane fitting of discs in Lupus, finding no obvious dependence on disc temperature.

So for nearby discs, the host star heating only affects the very inner regions and it does seem reasonable to estimate the disc mass using the cooler temperature that corresponds to the bulk of the disc mass. However, this overlooks the possible warming of dust in the outer disc due to nearby *external* sources (particularly massive stars, of which there are none in the nearby regions such as Lupus that so many detailed studies of individual discs have focused on). If this is significant, it could mean that disc dust masses in the denser parts of massive clusters are actually being underestimated in surveys when a temperature of 20 K is assumed for all discs. The implications here could be important for understanding the statistical properties of discs in clusters. Furthermore, this external heating could also affect the locations (or even existence) of snow lines in the disc, as well as the nature of grain evolution and even the ability to introduce pressure bumps, which could all affect the planet formation process.

External irradiation has been modelled in strong radiation scenarios looking at the effect on the gas dynamics/proplyds (e.g. Henney & O'Dell 1999; Richling & Yorke 2000; García-Arredondo et al. 2001; Haworth & Clarke 2019). However these calculations are computationally expensive, usually focus on the dynamics, and when it comes to observables usually focus on the photodissociation region (PDR) and photoionised gas diagnostics. More intermediate/low FUV radiation fields have also been included in hydrostatic disc models, but with a view to how it affects factors like ionisation and CO photodesorption (e.g. Cleeves et al. 2013; Cleeves 2016) rather than the dust radiative equilibrium temperature. Champion et al. (2017) undertook 1D PDR models of proplyds using the MEUDON code, however in those they compute the dust temperature in the surface layers and the disc temperature is assumed to be uniformly 19.5 K. Robberto et al. (2002) also took a similar approach semi-analytically, considering the proplyd to be a spherical system with non-spherical external irradiation and internal heating by the host star, but again the focus was on the layers external to the circumstellar disc and their infrared emission. Sellek et al. (2020) studied the evolution of dust in discs with an external photoevaporative wind, where only small grains are entrained (Facchini et al. 2016), but assumed a temperature profile for the disc that is dominated by the central source. Ndugu et al. (2018) included a parameterised heating of the outer disc in planet population synthesis models, finding that heating due to the cluster environment is important for suppressing large populations of cold Jupiters, which are not observed (particularly at low metallicity). However, we are not aware of direct calculations of this heating and/or a discussion of the impact upon disc mass diagnostics and other attributes such as snow line locations.

Overall, external heating of the dust that remains in the circumstellar disc appears to have been broadly overlooked in favour of the smaller dust entrained in the envelope. Given that this is the region of any planet formation, it is important to understand the thermal properties of the disc, both for understanding the planet formation process there and for improving the accuracy of millimetre continuum mass estimates, which themselves give insight into the planet formation potential of discs in massive clusters. Doing so is the objective of this paper.

2 SIMPLE RADIATIVE EQUILIBRIUM MODEL

We take a quick first look at the possible impact of an external source by considering an extension to the classic optically thin radiative equilibrium expression using the bolometric luminosity of the host star and external source, similar to the approach taken by Tsamis et al. (2013) in estimating the dust temperature of ONC proplyds.

Assume that there is a circumstellar disc that is heated to the grain radiative equilibrium temperature by the central host star (luminosity L_H) and an external source (luminosity L_{ext}). Also assume that the disc is optically thin. The heating rate for a grain of radius r_d and albedo α at radial distance R from the host star with the external source at distance D is

$$H = A_H 4\pi r_d^2 \left(\frac{L_H}{4\pi R^2} + \frac{L_{ext}}{4\pi D^2} \right) (1-\alpha) \quad (5)$$

where A_H is the fraction of the spherical grain surface that is irradiated. In the case of a planar radiation field travelling through a medium with zero scattering $A_H = 1/2$ because only one side of the grain is irradiated. However, for a more general radiation field, or a planar field incident upon a scattering medium $A_H = 1$. We spend the time clarifying this because Monte Carlo radiative transfer codes (Lucy 1999) generally compute the averaged properties in each volume of a calculation, effectively setting $A_H = 1$. We assume that the heating only has a radial dependence on the contribution from the host star and that the external heating is uniform. Assuming both sources are blackbodies the heating term becomes

$$H = A_H 4\pi r_d^2 \sigma \left(\frac{R_H^2}{R^2} T_H^4 + \frac{R_{ext}^2}{D^2} T_{ext}^4 \right) (1-\alpha). \quad (6)$$

The cooling rate of spherical grains in the disc at temperatre T_d is

$$C = 4\pi r_d^2 \sigma T_d^4 \quad (7)$$

Equating the heating and cooling in radiative equilibrium

$$4\pi r_d^2 \sigma T_d^4 = A_H 4\pi r_d^2 \sigma \left(\frac{R_H^2}{R^2} T_H^4 + \frac{R_{ext}^2}{D^2} T_{ext}^4 \right) (1-\alpha) \quad (8)$$

gives a radial temperatue profile

$$T_d = A_H^{1/4} \left[\left(\frac{R_H}{R} \right)^2 T_H^4 + \left(\frac{R_{ext}}{D} \right)^2 T_{ext}^4 \right]^{1/4} (1-\alpha)^{1/4} \quad (9)$$

This is shown for a Trappist-1 type star at various distances from a star similar to θ^1C ($R = 10\,R_\odot, T = 39000$ K) in Figure 1.

For an ensemble of external sources this can be generalized to

$$T_d = A_H^{1/4} \left[\left(\frac{R_H}{R} \right)^2 T_H^4 + \sum_k \left(\frac{R_{ext,k}}{D_k} \right)^2 T_{ext,k}^4 \right]^{1/4} (1-\alpha)^{1/4}$$

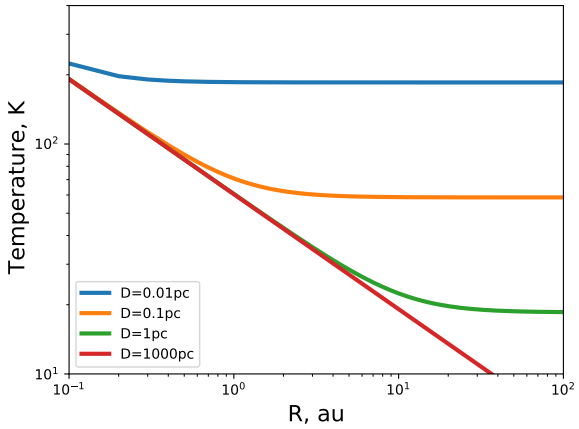

Figure 1. Analytic disc radiative equilibrium radial temperature profiles for a host star with $T_H = 2550$, $R_H = 0.121$ (Trappist-1) at various distances from a θ^1C analogue.

(10)

Note that in practice most discs will not be optically thin and the albedo is a function of wavelength and the grain size distribution.

The mass estimate given by equation 4 in the Rayleigh-Jeans regime scales inversely with the Temperature, so if assuming a temperature of 20 K the overestimate of the disc mass is by a factor $T_d/20$. If the external source dominates the bulk of the disc temperature this would hence lead to an overestimate that scales as $D^{-1/2}$.

3 RADIATIVE TRANSFER MODELS

To explore the dust temperature of externally irradiated discs in more detail we ran Monte Carlo radiative transfer calculations using the TORUS code (Harries et al. 2019). The approach used is based on that of Lucy (1999). The code uses an adapative mesh refinement grid-based approach, with a 2D cylindrical (R, z) grid geometry and the host star at the origin. The total source luminosity (host star plus any external source) is discretised into photon packets that undertake a physically motivated random walk over the grid until they escape. This contributes to the energy density in each cell which sets the dust temperature.

In these calculations, photon packets from the host star are emitted with random direction and a frequency randomly sampled from the stellar spectrum. When an external photon source is included, it is done so beyond the upper bound of the grid. External photons are hence introduced in a plane parallel fashion from the upper bound of the grid, with frequency again randomly sampled from the external sources spectrum. We choose this approach rather than an isotropic external source, since many irradiated discs close to massive stars are clearly not symmetrically irradiated. This way, we can ask questions like whether the external radiation field affects just the upper atmosphere, also the disc mid plane, or even the far side of the disc from the external radiation source. In this paper we only consider a plane parallel external field propagating parallel to the z axis on a cylindrical adaptive mesh refinement R, z grid, since there is a higher probability of the radiation impinging primarily upon the disc surface than the disc edge for a random disc orientation. Given that 3D models would be required for arbitrary external radiation orientations (otherwise you end up with what is effectively a cylindrical external source) we argue that this situation is the prudent choice.

3.1 Disc density distribution and dust properties

Our calculations will solve for the dust radiative equilibrium temperature, but density and grain distributions need to be specified.

We construct the disc using a truncated power law with a surface density profile

$$\Sigma(R) = \Sigma_{1\mathrm{au}} \left(\frac{R}{\mathrm{au}}\right)^{-1} \tag{11}$$

and scale height of the form

$$H(R) = H_{1\mathrm{au}} \left(\frac{R}{\mathrm{au}}\right)^{m} \tag{12}$$

where we choose $m = 1$. For such a surface density profile the mass encapsulated scales linearly with the radius, and the surface density normalization is given by

$$\Sigma_{1\mathrm{au}} = \frac{M_d}{2\pi R_d \times (1\,\mathrm{au})}. \tag{13}$$

The density structure on the cylindrical grid is then described by

$$\rho(R, z) = \frac{\Sigma(R)}{\sqrt{2\pi}H(R)} \exp\left(-\frac{z^2}{2H(R)^2}\right). \tag{14}$$

A summary of the parameters of discs for the models used in this paper is given in Table 1. For the exploration in this paper we use a single grain population. These are Draine & Lee (1984) silicates with a minimum and maximum grain size of 0.1 μm and 2 mm respectively. The power law of the $dn(a)/da \propto a^{-q}$ distribution is $q = 3.3$.

We do not solve for the hydrostatic equilibrium structure of the disc in these models. Rather, a parametric disc structure is imposed and the radiative equilibrium temperature calculated. We consider a few different values for the scale height at 1 au in the solar mass case, from the canonical $H/R = 0.1$ down to $H/R = 0.025$ to represent a more settled case. If optically thin the dust radiative equilibrium temperature of an isolated disc scales with the host star luminosity as $T_d \propto L_*^{1/4}$. At lower stellar masses we hence scale the imposed $H/R = 0.1$ by a factor

$$f_H = \left(\frac{L_*}{L_\odot}\right)^{1/8} \left(\frac{M_*}{M_\odot}\right)^{-1/2}. \tag{15}$$

We place each model star-disc at 1, 0.5, 0.1, 0.05 and 0.01 pc from a θ^1C analogue, with radius 10 $R_\odot$ and effective temperature of 39000 K. We also include an isolated version of each model disc with no external source.

3.2 Defining the sources

The stellar luminosity provides an additional complication because the pre-main sequence luminosity is a different function of time for different stellar masses and needs to be computed with a model such as those by Siess et al. (2000) or MESA (Paxton et al. 2011, 2013, 2015; Choi et al. 2016; Dotter 2016). In particular, before the zero age main sequence the luminosity is a shallower function of stellar mass. For this initial study we adopt stellar temperature and radii

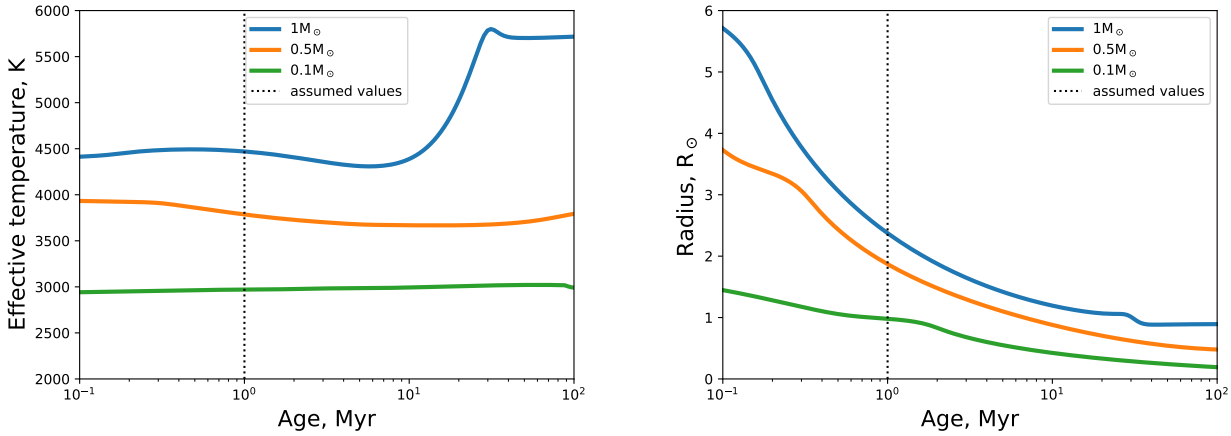

Figure 2. MIST v1.2 temperature and radius evolutionary tracks for stars of different masses. We use the values at 1 Myr (the vertical dotted line).

Stellar Mass ($M_\odot$)	T_* (K)	R_* ($R_\odot$)	R_d (au)	Σ_{1au} g cm^{-2}	Disc dust mass ($M_\oplus$)	H_{1au} (au)
1	4468	2.35	100	0.425	10.0	0.1
1	4468	2.35	100	0.425	10.0	0.05
1	4468	2.35	100	0.425	10.0	0.025
1	4468	2.35	50	0.851	10.0	0.1
1	4468	2.35	50	0.851	10.0	0.05
1	4468	2.35	50	0.851	10.0	0.01
1	4468	2.35	25	1.70	10.0	0.1
1	4468	2.35	10	4.25	10.0	0.1
0.5	3784	1.86	50	0.851	10.0	0.12
0.5	3784	1.86	25	1.70	10.0	0.12
0.5	3784	1.86	10	4.25	10.0	0.12
0.5	3784	1.86	10	2.12	5.0	0.12
0.5	3784	1.86	10	0.425	1.0	0.12
0.1	2970	0.98	50	0.851	10.0	0.21
0.1	2970	0.98	25	1.70	10.0	0.21
0.1	2970	0.98	10	4.25	10.0	0.21
0.1	2970	0.98	10	2.12	5.0	0.21
0.1	2970	0.98	10	0.425	1.0	0.21

Table 1. Summary of the star-disc properties of models in this paper. Each of these models are placed at different distances from an external UV source.

taken from MIST (v1.2) evolutionary tracks[1] at a time of 1Myr, assuming Fe/H = 0 and initial v/v$_{\rm crit}$ = 0.4. The adopted stellar temperatures and radii are shown in Figure 2 in the wider context of the stellar evolution. Table 1 also specifies the stellar parameters used.

An argument could be made about the short lifetimes of discs in close proximity to massive stars (the proplyd lifetime problem) but this problem is coupled to uncertainties on the disc properties, such as mass, age and time actually spent in the high UV environment. We therefore deem this choice of PMS stellar properties at a single age to be pragmatic and a much better representation of the probable reality than zero age main sequence luminosities.

There is a further consideration required, which is how to treat the external radiation field entering the 2D cylindrical grid. In section 3 we argued for treating this as a plane parallel field entering from the upper bound of the model grid. However, on a cylindrical grid the cylindrical area of a cell centred on R_i with thickness ΔR increases as

$$\Delta A = 2\pi \left[\left(R_i + \frac{\Delta R}{2} \right)^2 - \left(R_i - \frac{\Delta R}{2} \right)^2 \right] \quad (16)$$

so randomly introducing photon packets at the upper grid boundary with uniform probability in R would not correspond to a uniform planar field, but rather one with a density per unit area that decreases with R. To address this, the square root of the randomly sampled R/R_{grid} is used, where R_{grid} is the outermost radial coordinate of the grid.

The energy carried per photon packet ΔE is always the same, with different frequencies simply corresponding to different numbers of photons in the packet. For N packets and total source luminosity L the energy (per unit time) carried by a packet is $\delta E = L/N$. For the purpose of computing the photon packet energy, the luminosity of the external source, which is intrinsically $L_{ext,0}$, is scaled by

$$L_{ext} = L_{ext,0} \frac{\pi R_{grid}^2}{4\pi D_{grid}^2} \quad (17)$$

where R_{grid} is the radial grid size and D_{grid} is the distance of the external source from the grid.

3.3 Obvious caveats

Before proceeding to look at calculation results we note some of the obvious caveats with our approach to the modelling. This is not designed to be a detailed study of grain/disc evolution and planet formation, but rather a first look at the effect of external irradiation on the thermal structure of the circumstellar disc. To this end we consider only a single snapshot of any given disc. We consider a distribution of grain sizes that is the same everywhere (i.e. there is no midplane larger grain population and diffuse atmospheric population due to settling and/or entrainment of smaller grains in a wind). We also do not solve for hydrostatic equilibrium as when the external field is strong the disc will be being evaporated and a hydrostatic model is not necessarily better than a parametric dust structure. However, we do explore the impact of the the scale height of the dust which can be considered a rough proxy for settling. For

[1] http://waps.cfa.harvard.edu/MIST/interp$_t$*racks.html*

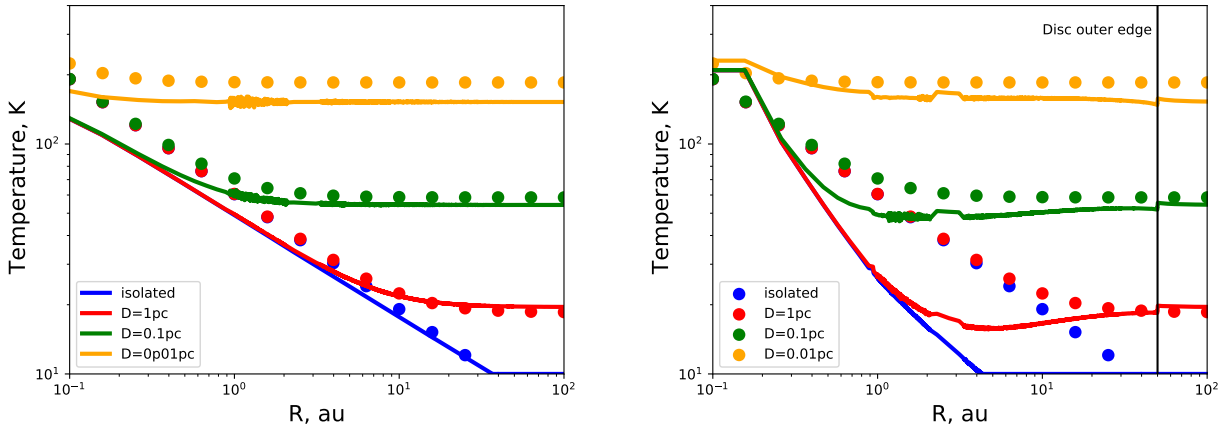

Figure 3. Points represent analytic disc radiative equilibrium radial temperature profiles for a host star with $T_H = 2550$, $R_H = 0.121$ (Trappist-1) at various distances from a star similar to θ^1C. The solid lines are results from TORUS radiative transfer models. The left hand panel is an extremely optically thin disc ($M_d = 10^{-17}$ M$_\oplus$) and the right hand panel is for a R_d =50 au, $M_d = 10$ M$_\oplus$ disc.

the systems in close proximity to a strong external radiation field we are assuming that the embedded dust is still geometrically disc-like, despite there being a larger scale proplyd structure. For this reason we do not explore synthetic SEDs in this paper, since the warm envelope makes an important contribution to the SED (e.g. Robberto et al. 2002; Champion et al. 2017). We will address the dynamic evolution of the dust in future work.

Another caveat is that although we consider a realistic pre main sequence stellar luminosity, we are not including the effects of accretion luminosity which may occasionally increase the heating from the central source.

3.4 Benchmarking in the optically thin regime

We begin by comparing TORUS against equation 9 in the extremely optically thin regime. We still use a disc model, as described above, only with a dust mass of 10^{-17} M$_\oplus$. In this first look we use host star properties similar to those of Trappist-1, i.e. $T_H = 2550$ K and $R_H = 0.121$ R$_\odot$ (though note that in our later calculations we use appropriate pre main sequence stellar properties from evolutionary models as described above) and the external source is similar to θ^1C (T_{ext}=39000 K, $R_{ext} = 10$ R$_\odot$).

A comparison of equation 9 and the mid-plane temperature of this extremely optically thin disc is shown in the left hand panel of Figure 3. The right hand panel is the same setup, only with the disc mass increased to a more typical value of 10 M$_\oplus$. For the analytic approximation in this case we assume a negligible albedo.

Overall the optically thin simulations give good agreement with the analytic solution, particularly beyond 10 au. When a more realistic disc mass is used the agreement is still good in the outer disc (dependent upon the distance of the disc from the radiation source). As expected, in the more realistic disc mass case the optically thick inner disc drops to a lower temperature value than equation 9 predicts.

We also study the deviation from the simple analytic solution in our other models in section 4.1, finding that the analytic approximation is typically good in the regions of the disc where the external field sets the temperature, but typically overestimates the disc temperature by a factor of around 4 where the host star dominates. Nevertheless equation 9 could still be used to place upper limits on the temperature and therefore corresponding lower limits on the disc mass.

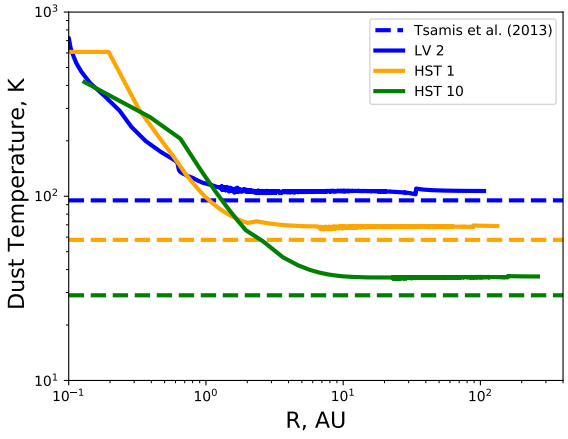

Figure 4. Comparison of our mid-plane dust temperature structure with the disc dust temperatures inferred by Tsamis et al. (2013) for the ONC proplyds LV2, HST 1 and HST 10. The agreement in the outer disc where the external radiation dominates is to within 20 per cent.

3.5 Testing against ONC proplyd disc temperature estimates

Tsamis et al. (2013) estimated the disc dust temperature of three proplyds in the ONC: LVC 2, HS1 and HST10. They also provided disc mass/radius estimates and the projected separation from θ^1 C. We used their disc/separation parameters, employing the host star parameters and canonical scale height at 1 au that we use for a 0.5 M$_\odot$ star (see table 1) to run comparison models of these systems.

The Tsamis et al. (2013) dust temperature estimates were made by assuming that 25 per cent of the θ^1 C bolometric luminosity reaches the disc surface. A comparison of their inferred dust temperatures with our model mid-plane dust temperature structure is given in Figure 4. In the outer disc where the external field dom-

inates the temperature the agreement is to within at worst 20 per cent.

4 RESULTS AND DISCUSSION

We begin by presenting the thermal structure of externally irradiated dust discs, before turning our attention to observables and effect upon disc dust mass estimates.

4.1 Thermal structure of internally and externally irradiated discs

Figure 5 shows the dust temperature structure of one of our model discs at different distances from a θ^1C-like external source. This scenario is a 0.5 $M_\odot$ host star with a 25 au, 10 $M_\oplus$ dust disc and the result is representative of the typical behaviour of our models. The upper left panel is an isolated disc, so there is no external radiation source, and illustrates the motivation for the usual assumption of a disc temperature of 20 K when computing disc mass estimates. The other panels from left to right, top to bottom, move the disc closer to an external radiation field, which is impinging from the upper boundary. This results in the upper half of the disc being warmer than the lower side, though the lower side is still heated relative to the isolated disc case. Since we only consider a static snapshot we do not assess the dynamical impact of this asymmetric heating here.

Figure 6 shows the mid-plane temperature of two of our star-disc models. In each case we include the isolated result, as well as at distances of 1, 0.1 and 0.01 pc from the external source. The models are M_d = 0.5 $M_\odot$, R_d = 25 au, M_d = 10 $M_\oplus$ (upper panel) and M_d = 1 $M_\odot$, R_d = 100 au, M_d = 10 $M_\oplus$ (lower panel), and are representative of the typical behaviour we see in all of the models. In addition to the model results (solid lines) we also include the analytic approximation given by equation 9 (dashed lines). For the discs nearest the external source (0.01 pc) the analytic approximation is reasonable but there is more significant deviation (a factor ~4) in the inner parts of the disc at larger separations when the external source doesn't set the disc temperature.

A key point to make here is that the disc temperature is in excess of the standard 20 K assumption once a disc is at a separation of less than a parsec from the θ^1 C like source. We will assess how this affects disc mass estimates in section 4.2, but note now that an upper limit on the temperature (which could be provided by the analytic approximation) corresponds to a lower limit on the inferred mass using equation 4, which is a valuable addition to an estimate made assuming a temperature of 20 K.

4.1.1 *Dependence of temperature structure on dust scale height*

The main calculations in this paper assume a single mixed grain population with small (0.1 μm) grains right the way through to 2 mm sized grains. In reality the larger grains settle towards the mid-plane. To make a simple assessment of the possible impact of this we ran calculations with smaller scale heights, but otherwise identical parameters (stellar properties, disc mass/radius).

A comparison of the mid-plane temperature structure of a canonical scale height model and others with a factor two and four smaller scale heights is given in Figure 7. The temperature of the outer parts of the disc heated by the external source doesn't change, but the radius at which the external source dominates (in the mid-plane at least) moves inwards. This is because the mid-plane is denser and so becomes optically thick to the host star radiation more quickly. However, the vertical column at any given radius (and hence to the external radiation) is the same.

There are two important points to make from this comparison. The first is that although we are considering a single density distribution for each model, there is only a finite amount of dust in the model so even if small grains are elevated away from the mid-plane we do not expect it to significantly affect the importance of external heating on the dust temperature (e.g. if the system were a proplyd). The second point is that what lifting dust away from the mid-plane may do is increase the ability of the host star to contribute to warming the disc (and vice-versa for settling).

4.1.2 *First comments on the effect of external irradiation upon snow lines*

Another important effect of external irradiation is the impact upon the locations (or even existence of) snow lines. The idea that planetary composition could link to formation locations in the disc through snow lines has been complicated in recent years due to factors like time dependent chemistry and pebble drift (Booth & Ilee 2019), thermal instability at snow lines (Owen 2020) and the time evolution of the host star luminosity (Miley et al. 2021). External irradiation adds yet another factor.

Here we do not study the time evolution of snow lines like e.g. Booth & Ilee (2019) and Miley et al. (2021), but in Figure 8 we show the radius in a 100 au, 10 $M_\oplus$ disc around a 1 $M_\odot$ star at which the temperature drops below certain values as a function of distance from the external radiation source. The rightmost set of points represent the thermal structure of an isolated disc (placed at 100 pc in Figure 8). Then moving left from this rightmost point one can follow how the location of particular mid-plane temperatures migrates outwards.

A temperature of 20 K roughly corresponds to the temperature of the CO snow line, 50 K is roughly the temperature of the CO_2 snow line and 150 K is roughly the temperature of the water snow line. The CO snow line moves outwards significantly compared to an isolated disc, doing so by a factor two even at separations of about a parsec from the O star. At closer separations, the CO snow line ceases to exist. The water snow line has been proposed as an important part of the planet forming mechanism for ensembles of planets on small orbits such as in Trappist-1 (Ormel et al. 2017; Schoonenberg et al. 2019). Naively based on our results we would anticipate that this would be rather resilient to the effect of the external irradiation as the water snow line is only significantly affected at separations of $\leq 10^{-2}$ pc. Of course even if the water snow line location isn't affected, the mass reservoir for planet formation could still be significantly affected by external photoevaporation (Haworth et al. 2018a).

4.2 Dust mass estimates

As dicussed above, disc dust masses are estimated via equation 4, restated here

$$M_d = \frac{D^2 F_\nu}{\kappa_\nu B_\nu(T)}$$

where D is the source distance, F_ν the measured flux, κ_ν the opacity and $B_\nu(T)$ the Planck function. In the Rayleigh-Jeans regime there is a linear scaling of the Planck function with the temperature, which is usually assumed to be around 20 K, motivated by the temperature structure of isolated discs. The significant additional heating from

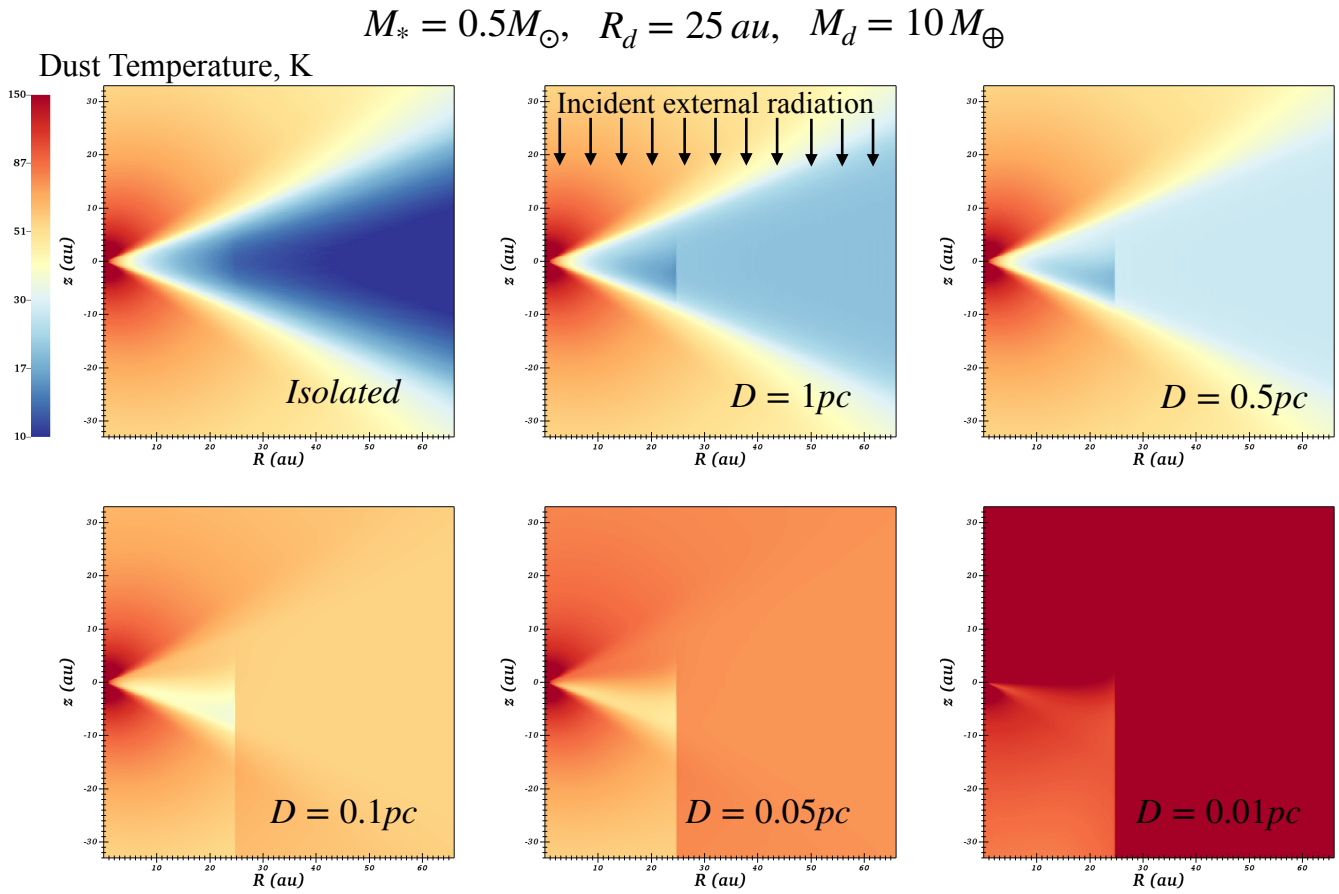

Figure 5. The dust radiative equilibrium temperature structure of a 10 $M_\oplus$ dust mass, 25 au disc around a 0.5 $M_\odot$ star at various distances from a 39000 K 10 $R_\odot$ star. The top left panel is isolated (no external source) and in the other panels the label in the lower right denotes the distance from the external source which irradiates the grid from the top part of each panel, as illustrated in the top-middle panel.

external sources considered here could therefore conceivably have an impact on the inferred disc mass, with the lower assumed temperature leading to overestimated disc dust masses. To test this we produce 850 μm synthetic observations from our calculations, again using the Monte Carlo radiative transfer approach in TORUS. When analysing these synthetic observations to estimate the dust mass that would be inferred we assume an opacity of $\kappa_\nu = 3.0588\,\mathrm{cm^2\,g^{-1}}$ at 850 μm (consistent with Eisner et al. 2018) and a distance of 414 pc. We do not account for any instrumentation effects such as finite beam size or interferometric effects as we are mostly interested in the impact of assuming a single temperature when computing the mass regardless of distance from the external source, which is insensitive to such factors.

Figure 9 shows the estimated dust masses as a function of projected separation from θ^1 C from Mann et al. (2014) and Eisner et al. (2018). Overplotted are a series of lines corresponding to the masses inferred from our synthetic observations, showing how the inferred disc mass changes for any given star-disc system as it is moved closer to the external source. As expected the inferred disc mass increases nearer to the external source due to the increased temperature, with an overestimate of the disc mass by a factor ~ 10 at a separation of 0.01 pc. We also find that the overestimate scales with distance from the external source as $D^{-1/2}$ as expected from the discussion in section 2, and significant deviations from the 20 K assumption start at about 1 pc (in this particular case). The $D^{-1/2}$ scaling interior to 1 pc is illustrated by the dotted line in Figure 9.

Ideally each individual source in the Mann et al. (2014) and Eisner et al. (2018) surveys would be subject to bespoke modelling, but for a first assessment of the possible impact of this bias we can simply scale the observed masses by the overestimate factor inferred from our models $f = (D/\mathrm{pc})^{-1/2}$, which we do in Figure 10. The upper panel shows the original data and the lower panel accounting for the temperature-induced overestimate of the disc mass by multiplying by the factor f. Of course there is uncertainty as to the true separation (since all we plot in Figure 10 is the projected separation), but our results suggest that a trend in disc mass with separation may be being suppressed.

It is worth noting that a trend in disc dust masses as a function of projected separation is not necessarily expected in an external photoevaporation scenario. The dynamical evolution of a star cluster on such small spatial scales is relatively fast, so any such signature might not survive very long. On the other hand it may also be quickly imprinted.

4.2.1 *Effect on other surveys?*

Here we have focused our attention on the ONC and θ^1 C. Another notable example of disc dust masses as a function of projected

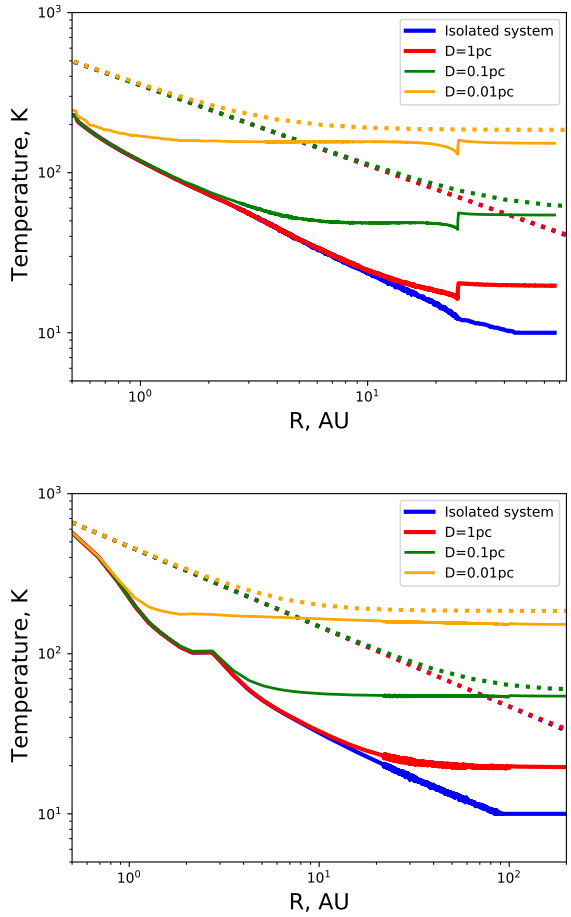

Figure 6. Mid-plane temperature profiles of externally irradiated disc models. The upper panel has a 0.5 $M_\odot$ host star, 25 au disc outer radius and 10 $M_\oplus$ of dust. The lower panel has a 1 $M_\odot$ host star, 100 au disc outer radius and 10 $M_\oplus$ of dust. The solid lines are the radiative transfer calculation results and the dotted lines are the simple analytic radiative equilibrium approximations.

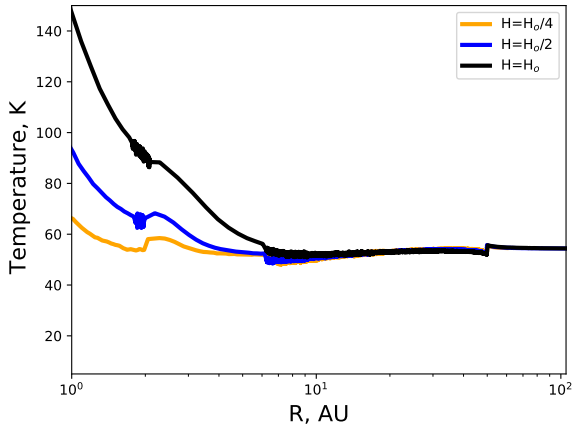

Figure 7. Mid-plane temperature profiles of externally irradiated disc models with different scale heights at a distance of 0.1 pc from the external source. A smaller scale height results in lower inner-disc temperatures, with the external radiation field dominating the mid-plane temperature at smaller distances from the host star. This is because the mid-plane is more optically thick to the host-star radiation, but the overall vertical column is unchanged.

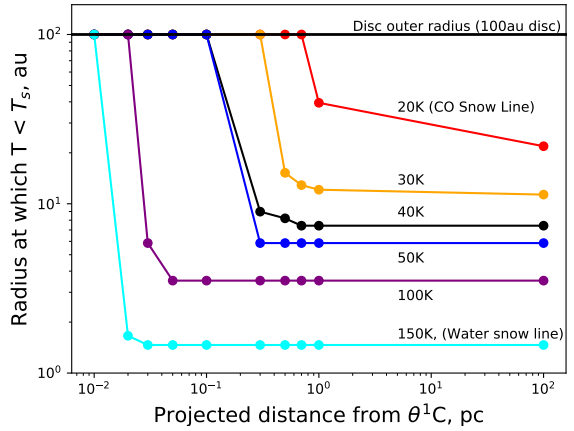

Figure 8. The radius at which certain temperatures are reached in the disc mid-plane. For example the CO snow line is at 22 au until about 1 pc distance from a θ^1C analogue, but at closer distances no CO snow line would exist. The water snow line, of possible importance to inner planet formation, is relatively unaffected by environment except for at very close separations. This is for a 100 au disc with a 10 $M_\oplus$ dust mass and $H/R = 0.1$

separation is in the older σ Orionis cluster by Ansdell et al. (2017), where an increase in disc dust mass as a function of projected separation from σ Ori was observed. However, their trend was at distances of more like beyond a parsec from σ Ori and the luminosity of σ Ori is also about a factor 5 weaker than θ^1 C. We hence expect any overestimate of disc masses due to external heating plays a much weaker role in that region. van Terwisga et al. (2020) also surveyed disc masses with ALMA towards NGC 2024. There are a number of discs in close (projected) proximity to IRS 2b in that region, so external heating of dust discs and the corresponding effect on disc mass estimates could well be having an impact in that region. However IRS 2b is again less luminous than θ^1 C.

4.2.2 *Effect of disc inclination.*

Estimating disc dust masses using equation 4 assumes that the emission is optically thin, in which case there should not be a sensitivity to inclination. If the disc were optically thick then the situation becomes substantially more complicated. On the one hand the disc mass may be being underestimated if it is optically thick. The disc mass inferred would then also be sensitive to the disc inclination, since if the warmer irradiated side were presented to the observer the emission would be brighter and (if a temperature of 20 K were assumed) some of the mass estimate deficit from being optically thick accounted for. Conversely if the cold side were presented the inferred mass would be lower. For simplicity it is best to assume that the disc is generally optically thin and consider the inclination/optical depth effects when undertaking bespoke modelling of individual discs.

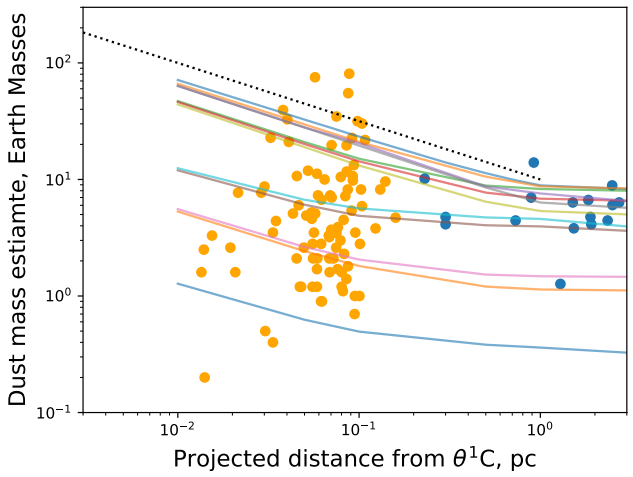

Figure 9. Inferred disc 850 μm dust masses as a function of projected separation from $\theta^1 C$. The blue points are detections (we ignore upper limits here) from Mann et al. (2014) and the orange points are detections from Eisner et al. (2018). The solid coloured lines are TORUS radiative equilibrium synthetic 850 μm models, with tracks representing an identical star-disc, just at different distances from the external radiation source. As the star-disc approaches the massive external source the mass of the dust disc is overestimated when assuming a temperature of 20 K, since the true dust temperature is in fact higher. The dotted line denotes a $D^{-1/2}$ scaling.

4.3 Possible effect on grain evolution and planet formation

So far we have focused on the effect that the increased disc dust temperature has on continuum mass estimates and commented on the effect on snow lines. It is also worth briefly considering the possible impact of higher disc dust temperatures and a flatter radial temperature profile on grain evolution.

Firstly and most simply, our results indirectly support the work of Ndugu et al. (2018), where higher outer disc temperatures were imposed in planet population synthesis models. They found that this outer heating is important for suppressing populations of cold Jupiters, particularly at low metallicity, which are not observed.

We can also consider the impact of externally heated disc temperature structures on grain growth and drift following the simple model of Birnstiel et al. (2012). For example the drift timescale and maximum grain size before the onset of radial drift both scale inversely with the square of the sound speed and log pressure gradient ($|\mathrm{d}\ln(P)/\mathrm{d}\ln(R)|$). For a heated irradiated disc both of these quantities will be decreased by a factor $T_{\rm isolated}/T_{\rm irradiated}$ due to the change in sound speed. Since the temperature profile in the externally heated disc is much flatter, the reduced log pressure gradient will also act to slightly further reduce the drift timescale and maximum grain size for drift. So overall drift may happen to smaller grains, and more rapidly. Whether this helps to promote or further hinder planet formation (in addition to the photoevaporative depletion of the disc) remains to be explored.

Another factor is that the Stokes number (grain size) for fragmentation of grains through collisions scales inversely with the temperature, so the Stokes number/size for fragmentation will be decreased by a factor $T_{\rm isolated}/T_{\rm irradiated}$ in a warmed irradiated disc. Once again, this could act to further suppress planet formation in tandem with the removal of material by external photoevaporation.

Finally is worth noting that if the disc temperature distribution is flatter (as it is in the bulk of an irradiated disc) then it is easier to introduce pressure bumps through density perturbations which could lead to dust trapping.

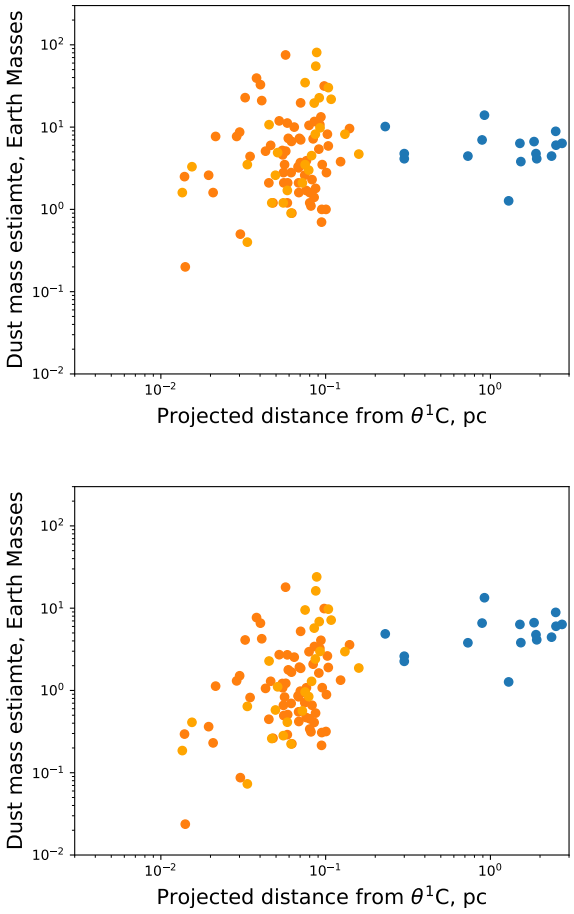

Figure 10. Inferred disc dust masses as a function of projected separation from $\theta 1C$. The upper panel is a combination of the detections (we ignore upper limits here) from Mann et al. (2014) (blue points) and Eisner et al. (2018) (orange points). The lower panel is scaled by the $(D/\mathrm{pc})^{0.5}$ factor by which our models suggests the masses are being overestimated.

5 SUMMARY AND CONCLUSIONS

We use Monte Carlo radiative transfer models to study the radiative equilibrium structure of protoplanetary discs irradiated by both the host star and an external source. We draw the following main conclusions from this work.

1) The majority of the dust component of discs in the vicinity of massive stars can be heated by the external radiation field to well in excess of the 20 K usually assumed (even in dense clusters) for estimating disc masses. This leads to disc masses being overestimated when assuming a 20 K disc, since warmer discs are brighter. The overestimate scales with the separation from the external source as roughly $D^{-1/2}$, until the disc is sufficiently far from the external source that the host star just dominates the temperature structure. In the vicinity of θ^1C in the ONC the

external field starts to play an important role at a separation of about a parsec and results in roughly a factor 10 overestimate on the dust mass at separations of 0.01 pc.

2) Applying a simple $D^{-1/2}$ scaling to observed disc dust masses as a function of projected separation from θ^1C results in a significantly stronger variation in disc mass with projected separation. Though of course this has the caveat that projected separation is not necessarily the true separation. Bespoke models of ONC discs on a case-by-case basis would be required for a more rigorous assessment of the impact of external heating on disc mass estimates.

3) External heating is able to affect mid-plane snow line locations, which further complicates the idea of being able to relate planet compositions to formation radii. The CO snow line is quite readily removed completely from discs near massive stars, whereas the water snow line (which may be important for inner planet formation) is resilient to cluster heating except for very small separations (≤ 0.01 pc) from a θ^1C type external source

ACKNOWLEDGEMENTS

We thank Andrew Sellek and Will Henney for useful discussions. TJH is funded by a Royal Society Dorothy Hodgkin Fellowship. This work used the DiRAC@Durham facility managed by the Institute for Computational Cosmology on behalf of the STFC DiRAC HPC Facility (www.dirac.ac.uk). The equipment was funded by BEIS capital funding via STFC capital grants ST/P002293/1, ST/R002371/1 and ST/S002502/1, Durham University and STFC operations grant ST/R000832/1. DiRAC is part of the National e-Infrastructure.

This paper has been typeset from a TEX/LATEX file prepared by the author.

REFERENCES

Ansdell M., Williams J. P., Manara C. F., Miotello A., Facchini S., van der Marel N., Testi L., van Dishoeck E. F., 2017, AJ, 153, 240
Ansdell M., et al., 2020, AJ, 160, 248
Birnstiel T., Klahr H., Ercolano B., 2012, A&A, 539, A148
Booth R. A., Ilee J. D., 2019, MNRAS, 487, 3998
Boyden R. D., Eisner J. A., 2020, ApJ, 894, 74
Champion J., Berné O., Vicente S., Kamp I., Le Petit F., Gusdorf A., Joblin C., Goicoechea J. R., 2017, A&A, 604, A69
Choi J., Dotter A., Conroy C., Cantiello M., Paxton B., Johnson B. D., 2016, ApJ, 823, 102
Cleeves L. I., 2016, ApJ, 816, L21
Cleeves L. I., Adams F. C., Bergin E. A., 2013, ApJ, 772, 5
Concha-Ramírez F., Wilhelm M. J. C., Portegies Zwart S., Haworth T. J., 2019, MNRAS, 490, 5678
Dotter A., 2016, ApJS, 222, 8
Draine B. T., Lee H. M., 1984, ApJ, 285, 89
Eisner J. A., et al., 2018, ApJ, 860, 77
Facchini S., Clarke C. J., Bisbas T. G., 2016, MNRAS, 457, 3593
García-Arredondo F., Henney W. J., Arthur S. J., 2001, ApJ, 561, 830
Harries T. J., Haworth T. J., Acreman D., Ali A., Douglas T., 2019, Astronomy and Computing, 27, 63
Haworth T. J., Clarke C. J., 2019, MNRAS, 485, 3895
Haworth T. J., Facchini S., Clarke C. J., Mohanty S., 2018a, MNRAS, 475, 5460
Haworth T. J., Clarke C. J., Rahman W., Winter A. J., Facchini S., 2018b, MNRAS, 481, 452
Haworth T. J., Kim J. S., Winter A. J., Hines D. C., Clarke C. J., Sellek A. D., Ballabio G., Stapelfeldt K. R., 2020, MNRAS,
Henney W. J., O'Dell C. R., 1999, AJ, 118, 2350
Kim J. S., Clarke C. J., Fang M., Facchini S., 2016, ApJ, 826, L15
Kurtovic N. T., et al., 2018, ApJ, 869, L44
Lichtenberg T., Golabek G. J., Burn R., Meyer M. R., Alibert Y., Gerya T. V., Mordasini C., 2019, Nature Astronomy, 3, 307
Lucy L. B., 1999, A&A, 344, 282
Mann R. K., et al., 2014, ApJ, 784, 82
Miley J. M., Panić O., Booth R. A., Ilee J. D., Ida S., Kunitomo M., 2021, MNRAS, 500, 4658
Ndugu N., Bitsch B., Jurua E., 2018, MNRAS, 474, 886
Nicholson R. B., Parker R. J., Church R. P., Davies M. B., Fearon N. M., Walton S. R. J., 2019, MNRAS, 485, 4893
O'dell C. R., Wen Z., 1994, ApJ, 436, 194
Ormel C. W., Liu B., Schoonenberg D., 2017, A&A, 604, A1
Owen J. E., 2020, MNRAS, 495, 3160
Paxton B., Bildsten L., Dotter A., Herwig F., Lesaffre P., Timmes F., 2011, ApJS, 192, 3
Paxton B., et al., 2013, ApJS, 208, 4
Paxton B., et al., 2015, ApJS, 220, 15
Reiter M., 2020, A&A, 644, L1
Richling S., Yorke H. W., 2000, ApJ, 539, 258
Robberto M., Beckwith S. V. W., Panagia N., 2002, ApJ, 578, 897
Rodriguez J. E., et al., 2018, ApJ, 859, 150
Scally A., Clarke C., 2001, MNRAS, 325, 449
Schoonenberg D., Liu B., Ormel C. W., Dorn C., 2019, A&A, 627, A149
Sellek A. D., Booth R. A., Clarke C. J., 2020, MNRAS, 492, 1279
Siess L., Dufour E., Forestini M., 2000, A&A, 358, 593
Tazzari M., et al., 2017, A&A, 606, A88
Tsamis Y. G., Flores-Fajardo N., Henney W. J., Walsh J. R., Mesa-Delgado A., 2013, MNRAS, 430, 3406
Winter A. J., Clarke C. J., Rosotti G., Ih J., Facchini S., Haworth T. J., 2018, MNRAS, 478, 2700
Winter A. J., Kruijssen J. M. D., Longmore S. N., Chevance M., 2020, Nature, 586, 528
van Terwisga S. E., et al., 2020, A&A, 640, A27